Comparative Biochemistry and Physiology, Part B 257 (2022) 110678

Contents lists available at ScienceDirect

Comparative Biochemistry and Physiology, Part B

journal homepage: www.elsevier.com/locate/cbpb

De novo transcriptome assemblies of red king crab (*Paralithodes camtschaticus*) and snow crab (*Chionoecetes opilio*) molting gland and eyestalk ganglia - Temperature effects on expression of molting and growth regulatory genes in adult red king crab

Øivind Andersen [a,b,*], Hanne Johnsen [a,c,1], Astrid C. Wittmann [d,e,1], Lars Harms [e], Tina Thesslund [a], Ragnhild Stenberg Berg [a], Sten Siikavuopio [a], Donald L. Mykles [f,g]

[a] Nofima, Tromsø NO-9291, Norway
[b] Department of Animal and Aquacultural Sciences (IHA), Faculty of Life Sciences (BIOVIT), Norwegian University of Life Sciences (NMBU), PO Box 5003, 1433 Ås, Norway
[c] Norwegian Polar Institute, 9296 Tromsø, Norway
[d] MARUM - Center for Marine Environmental Sciences, University of Bremen, 28359 Bremen, Germany
[e] Alfred Wegener Institute, Helmholtz Centre for Polar and Marine Research, 27570 Bremerhaven, Germany
[f] Department of Biology, Colorado State University, Fort Collins, CO 80523, USA
[g] Bodega Marine Laboratory, University of California, Davis, Bodega Bay, CA 94923, USA

ARTICLE INFO

Editor: Chris Moyes

Keywords:
Halloween genes
Anomura
Y-organ
Ecdysteroids
Thermal acclimation

ABSTRACT

Red king crab (*Paralithodes camtschaticus*) and snow crab (*Chionoecetes opilio*) are deep-sea crustaceans widely distributed in the North Pacific and Northwest Atlantic Oceans. These giant predators have invaded the Barents Sea over the past decades, and climate-driven temperature changes may influence their distribution and abundance in the sub-Arctic region. Molting and growth in crustaceans are strongly affected by temperature, but the underlying molecular mechanisms are little known, particularly in cold-water species. Here, we describe multiple regulatory factors in the two high-latitude crabs by developing *de novo* transcriptomes from the molting gland (Y-organ or YO) and eye stalk ganglia (ESG), in addition to the hepatopancreas and claw muscle of red king crab. The Halloween genes encoding the ecdysteroidogenic enzymes were expressed in YO, and the ESG contained multiple neuropeptides, including molt-inhibiting hormone (MIH), crustacean hyperglycemic hormone (CHH), and ion-transport peptide (ITP). Both crabs expressed a diversity of growth-related factors, such as mTOR, AKT, Rheb and AMPKα, and stress-responsive factors, including multiple heat shock proteins (HSPs). Temperature effects on the expression of key regulatory genes were quantified by qPCR in adult red king crab males kept at 4 °C or 10 °C for two weeks during intermolt. The Halloween genes tended to be upregulated in YO at high temperature, while the ecdysteroid receptor and several growth regulators showed tissue-specific responses to elevated temperature. Constitutive and heat-inducible HSPs were expressed in an inverse temperature-dependent manner, suggesting that adult red king crabs can acclimate to increased water temperatures.

1. Introduction

Red king crab and snow crab are giant deep-sea predators in the benthic ecosystems of sub-Arctic regions in the North Pacific and North Atlantic Oceans. Red king crab is among the world's largest arthropods attaining weights up to 11 kg and with legs spanning 1.8 m, while snow crab is slightly smaller (Stevens, 2014). They are highly important commercial fisheries resources, and both species have established non-native populations in the Barents Sea. Snow crabs inhabit depths down to 1400 m at temperatures from −1.5 °C to 4 °C year-round (Squires, 1990; Dawe and Colbourne, 2002), while red king crabs occur at depths down to 400 m in the Barents Sea with temperatures ranging

* Corresponding author at: Nofima, Tromsø NO-9291, Norway.
E-mail address: oivind.andersen@nofima.no (Ø. Andersen).
[1] These authors contributed equally to this work.

https://doi.org/10.1016/j.cbpb.2021.110678
Received 3 May 2021; Received in revised form 16 September 2021; Accepted 8 October 2021
Available online 14 October 2021

from below freezing to about 8 °C (Stiansen et al., 2009). Adult snow and king crabs showed behavioral thermoregulation in laboratory experiments by selecting the coldest end (1.5–3.5 °C) of the temperature gradient (Christiansen et al., 2015; Siikavuopio et al., 2019). Increased abundance and spread of the two invasive crab species may have great impact on the native life in the sub-Arctic region in the future (Jørgensen and Primicerio, 2007; Oug et al., 2011; Falk-Petersen et al., 2011). Changes in abundance and biodiversity relate to temperature changes and variability, as well as to predation and fishing pressure (Dvoretsky and Dvoretsky, 2016, 2020; Green et al., 2014; Poloczanska et al., 2016; Quinn, 2017; Scheffers et al., 2016). Ectotherms will only grow in the thermal range in which energy supply from aerobic metabolism is higher than the maintenance costs (Pörtner and Knust, 2007; Pörtner, 2010; Sokolova et al., 2012). The energy budget in snow crab seems to become negative above 7 °C due to reduced feeding and rising metabolic costs, and adult red king crab males kept at 4 °C, 8 °C or 12 °C for 110 days showed higher food conversion efficiency at the lowest temperature and higher mortality at elevated temperatures (Foyle et al., 1989; Thompson and Hawryluk, 1990; Siikavuopio et al., 2017). Temperature is a major external factor influencing physiological rates, growth and molting in crustaceans (Hartnoll, 1982, 2001; Anger et al., 2003; Wittmann et al., 2011, 2012, 2018). Juvenile red king crabs showed increased growth up to 15 °C and an inverse exponential relationship between intermolt period and temperature up to 12 °C (Stoner et al., 2010; Long and Daly, 2017). Similarly, intermolt period was shorter at 8 °C than at 3 °C in juvenile snow crabs (Yamamoto et al., 2015).

The cyclic shedding of the chitinous exoskeleton is essential for growth and development in crustaceans. Molting is regulated by complex interactions between conserved neuropeptides produced in the eyestalk ganglia (ESG) and molting hormones (ecdysteroids) secreted from the paired molting glands, or Y-organs (YO), situated in the anterior cephalothorax (Mykles, 2011; Mykles and Chang, 2020). During intermolt, the synthesis and secretion of ecdysteroids are inhibited by the pulsatile release of molt-inhibiting hormone (MIH) and crustacean hyperglycemic hormone (CHH) from the X-organ-sinus gland complex in the ESG, while the reduced levels of circulating MIH at early premolt induces hypertrophy of YO and activates ecdysteroid synthesis (Mykles and Chang, 2020). The pleiotropic CHH exerts an inhibitory effect on molting and reproduction, but also plays a role in the acute response to environmental stressors (Webster, 1996; Lorenzon et al., 2004; Fanjul-Moles, 2006). Dietary cholesterol is converted to ecdysteroids through a series of catalytic reactions involving the Rieske-oxygenase Neverland (Nvd) and five cytochrome P450 (CYP450) monooxygenases encoded by the Halloween genes *spook* (CYP307A1), *phantom* (CYP306A1), *disembodied* (CYP302A1), *shadow* (CYP315A1), and *shade* (CYP314A1) or *shed* (CYP314A1) (Mykles, 2011; Goody et al., 2014; Qu et al., 2015; Ventura et al., 2017; Swall et al., 2021). The upregulated ecdysteroid synthesis at premolt is associated with increased expression of the ecdysteroid receptor (EcR), which forms a functional heterodimer with the retinoid x receptor (RXR) (Yao et al., 1993; Chung et al., 1998).

Tissue growth is regulated by the highly conserved mechanistic Target of Rapamycin (mTOR) controlling protein synthesis and gene expression in response to nutrients, growth factors, and stressors (Saxton and Sabatini, 2017; Liu and Sabatini, 2020). mTOR activity is required for ecdysteroidogenesis and up-regulates ecdysteroid biosynthetic genes in the YO (Mykles and Chang, 2020; Shyamal et al., 2018). An activating key regulator of mTOR is Ras homolog enriched in brain (Rheb), and molting increases *Rheb* mRNA levels in the YO (Das et al., 2018; Shyamal et al., 2018; Wittmann et al., 2018). Rheb is controlled by the inhibitory tuberous sclerosis complex (TSC1/2), which in turn is inhibited by AKT (also known as protein kinase B) and activated by AMP kinase (AMPK) (Saxton and Sabatini, 2017; Liu and Sabatini, 2020).

Red king crab and snow crab belong to the suborders Anomura ("half" crabs) and Brachyura ("true" crabs), respectively, which diverged about 325 million years ago (Wolfe et al., 2019). These crabs are excellent models for understanding how climate change and associated water temperature changes may influence important physiological processes in cold-water crustaceans. The planktonic larvae of red king crab tolerate a wide range of temperatures, and larvae acclimated to 14 °C displayed higher tolerance to warm challenge temperatures compared to those reared at 4 °C or 8 °C (Michelsen et al., 2019). Juvenile red king crabs showed strong compensatory shifts in gene expression in response to acclimation to 10.5 °C, 12.5 °C or 14.5 °C in a transcriptome-wide whole organism study (Stillman et al., 2020). Similar growth in adult red king crabs kept at 4 °C, 8 °C or 12 °C (Siikavuopio and James, 2015) suggests that adults are also capable to acclimate to a wide range of temperatures, but the underlying compensatory mechanisms on tissue level are unknown. Genomic resources from the two species have recently become available in studies of transcriptomic response to seismic surveying noise in snow crab hepatopancreas (Hall et al., 2020) and to decreased pH and elevated temperature in whole pre-adults and in heart, gill and integument of adult red king crabs (Stillman et al., 2020). Here, we generated *de novo* transcriptome assemblies from the YO and ESG in both species and from hepatopancreas and claw muscle in red king crab. Multiple regulatory, molt-related, and endocrine factors were for the first time described in the two crab species. Expression of mTOR signaling, Halloween, *EcR* and *hsp* genes were measured by real-time quantitative polymerase chain reaction (qPCR) in YO, ESG, hepatopancreas and claw muscle of male red king crabs in intermolt kept at 4 °C or 10 °C for 14 days to study how a cold-water crab copes with exposure to elevated temperature.

2. Materials and methods

2.1. Animals

Adult red king crabs were caught by local fishermen in the sea off Varangerfjorden in Finnmark county, Norway and transported to the Aquaculture research station at Kårvika Research Station, Tromsø, Norway in January 2018. The crabs were held in two 3 m^2 (900 l) tanks each divided into four 0.75 m^2 compartments with their own water inlet at ambient temperature (2.5–4.0 °C) under natural light and photoperiod. Adult male snow crabs were caught in the Bering Sea late autumn 2017 and transported to the Station where they were kept in round tanks (1.75 m^2) with shaded natural light and a water temperature ranging between 2.0 and 3.8 °C. Both species were fed in excess with pollock, herring and blue mussel three times weekly. Before sample collection, crabs were anaesthetized with clove oil (0.125 ml/l seawater, NOW Foods, USA) and sacrificed by an incision of the supraesophageal ganglion (brain).

For generating transcriptome assemblies, YO and ESG were collected from one snow crab in intermolt stage at 10. Feb. 2018 and stored in RNAlater (Ambion, 1:10 volume ratio) at −20 °C after 4 °C overnight. Putative YO, ESG, hepatopancreas and major claw muscle were dissected from two male red king crabs in early and late premolt stages at 21. Feb. and 13. March 2018, respectively. Several putative YO-containing tissues were collected and bisected with one part fixed in 10% formalin (Kemetyl) and the other submerged in RNAlater, which was also used for securing the other tissue samples.

For the temperature experiment, a total of 56 male red king crabs in postmolt were acclimated to 4 °C for 11 weeks in the two tanks described above. It should be noted that the water supply to both tanks was accidently disturbed for a few hours six days before the first sampling (T0) that caused a temperature drop. At 25. April 2018 eight crabs were collected from both tanks and sacrificed before samples were secured as described above. The water temperature in one of the tanks was then kept at 4 °C, while the other tank was raised to 10 °C by increasing the temperature with 1 degree per day. After 14 days at 4 °C or 10 °C, eight crabs were sacrificed and samples were dissected at 15. May 2018 (T1).

2.2. Molt-staging

Molt cycle stages were determined by inspection of the cuticle thickness and setal development of scaphognathites (Moriyasu and Mallet, 1986). They were dissected and submerged in crab saline (430 mM NaCl, 5 mM K_2SO_4, 7 mM $MgCl_2$, 4.5 mM, $CaCl_2$, and 10 mM Hepes–NaOH; pH 7.2, Lee et al., 2007) and kept at 4 °C for at least 24 h before analysis using light microscopy (Nikon Eclipse Ci) and the Nikon Nis-Elements Basic Research software.

2.3. Histology

Formalin-fixed putative YO tissues were processed overnight in Tissue Processor (Logos, Milestone). Paraffin embedded tissues were sectioned (2 μm) using a rotary microtome (Leica) and stained with hematoxylin and eosin (Merck) in auto-stainer (Leica) at the Norwegian Veterinary Institute, Harstad. All slides were then analyzed at Nofima, Tromsø, using light microscopy (Nikon Eclipse Ci) and the Nikon Nis-Elements Basic Research software. Candidate YO specific cells were verified by transcriptome analysis of parallel samples stored in RNAlater.

2.4. RNA extraction and transcriptome analyses

Total RNA was isolated from two putative YO samples (localization see Fig. 1B), ESG, major claw muscle and hepatopancreas dissected from two red king crabs at early and late premolt stage, and from the YO and ESG of one snow crab in intermolt using AllPrep DNA/RNA/miRNA Universal Kit (Qiagen) according to the manufacturer's protocol. RNA quality and quantity were determined using NanoDrop 8000 (Thermo Scientific) and Bioanalyzer (Agilent). A260/280 and A260/230 ranged from 1.93–2.22 to 0.95–1.96, respectively, while RIN values ranged from 5 to 10. It is known that RNA of arthropods is inclined to appear degraded using Bioanalyzer due to a gap deletion of 28S ribosomal RNA (rRNA) subunit (McCarthy et al., 2015; DeLeo et al., 2018). Thus, heat-denatured and untreated samples were analyzed using the Bioanalyzer. Ten samples were shipped to the Norwegian Sequencing Centre, Oslo, Norway, for Illumina sequencing. Briefly, libraries were prepared using a Strand-specific TruSeq RNA-seq library prep kit (Illumina), and paired-ends sequenced using a HiSeq 3/4000 Genome Analyser (Illumina), in one lane with a read length of 150 bp.

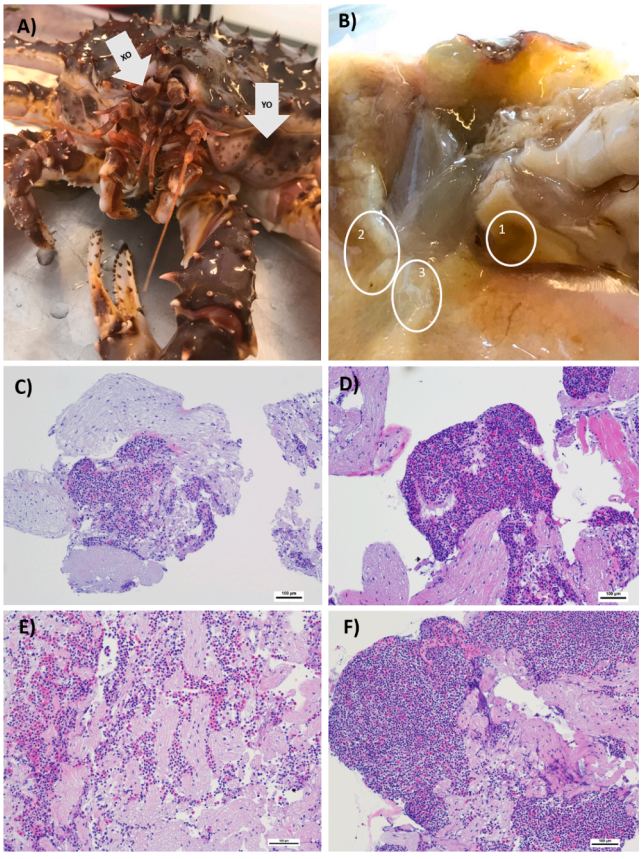

Fig. 1. Identification of Y-organ (YO) in red king crab. A) Localization of YO in the fused segments of the mouthparts and of the paired X-organ (XO) in the eyestalks. B) The three areas included in the search for YO. C-F) Histology of glandular tissue in YO. C) KingCrab16_YO2, area #1 sample 2. D) KingCrab16_YO3, area #1 sample 3. E) KingCrab 20_YO1, area #1. F) KingCrab20_YO2, area #2. Scale bar 100 μm. (For interpretation of the references to colour in this figure legend, the reader is referred to the web version of this article.)

Raw reads were quality controlled by FastQC v. 0.11.7 (Babraham Institute, Cambridge, UK). Adapter sequences were removed with bbduk.sh, from the BBtools suite, version 38.01 (Bushnell, 2015) with following parameters: ktrim = r, k = 23, mink = 11, hdist = 1, tpe, tbo. Remaining sequences were checked for rRNA sequences by SortMeRNA version 2.1 (Kopylova et al., 2012) and removed before further processing. To filter the sequences for the common Illumina spikein PhiX, bbduk.sh was used with a kmer size of 31 and a hdist of 1. A final quality trimming was performed with bbduk.sh using Q10 as minimum quality and 36 bases as the minimum length. All obtained sequences were normalized using bbnorm.sh (Bushnell, 2015) with an average depth of 200× and a minimum depth of 5× before they were *de novo* assembled using the Trinity genome-independent transcriptome assembler (release 2.6.6; (Grabherr et al., 2011) with a minimum transcript length of 300 bases and the option for strand specificity set (−-SS_lib_type RF). For each of the king crabs separate assemblies of claw muscle and putative YO tissues (two samples per animal) were generated (Table 1; KingCrab16_MC, KingCrab16_YO2, KingCrab16_YO3, KingCrab20_MC, KingCrab20_YO1, KingCrab20_YO2. KingCrab16_YO2, KingCrab16_YO3 and KingCrab20_YO1 were sampled from Area #1 and KingCrab20_YO2 was sampled from Area #2, see Fig. 1B), as well as assemblies that contained all reads from all the tissues of one individual (KingCrab16 and KingCrab20). Furthermore, reads of both individuals were combined to a comprehensive assembly (KingCrab16_20). For the snow crab, one assembly, which contained reads from YO only (SnowCrab9_YOa) and one of YO and ESG combined were generated (SnowCrab9). The read representations of the assemblies were assessed using the Bowtie2 2.3.4.1 software. The completeness was evaluated using the package BUSCO v3.0.0 (Benchmarking Universal Single-Copy Orthologs) and the orthologs of the public database"Arthropoda_odb9 (1066)". The annotation of the *de novo* assembled transcriptomes was performed using the Trinotate functional annotation suite (v 3.1.1; (Grabherr et al., 2011), including homology searches against the UniProt Swiss-Prot and NCBI non-redundant databases. MEtaGenome ANalyzer (MEGAN Community Edition, version 6.20.17) was used to explore eggNOG and KEGG pathway assignments and test for similarity among tissue-specific assignments of KEGG proteins by generating an UPGMA tree using the Bray-Curtis method.

Halloween gene transcripts in the king crab and snow crab assemblies were identified by a local blastn against *Gecarcinus lateralis* sequences (Benrabaa, 2019; Swall et al., 2021; Supplementary Table S2). Once available, text searches within the annotation results were done to identify assembled sequences of Halloween genes and other genes of interest for qPCR and construction of phylogenetic trees.

Multiple peptide sequences were imported to MEGA X (Kumar et al., 2018) and aligned using MUSCLE (Edgar, 2004). The analyses were conducted using the Maximum Likelihood method. The best model for each alignment was chosen using the ML option (Find the best DNA/protein models) provided by the software. Models with the lowest BIC scores (Bayesian Information Criterion) are considered to describe the substitution pattern the best. Based on the BIC values the LG (+G + I)

Table 1

Assembly	Tissue types	Total number of genes	Total number of transcripts	Median length (N_{50}) of transcripts (bp)	Mean length (bp)	Total number of assembled bases	Overall alignment rate (%)	Number of NR hits (genes)	Number of SP hits (genes)	Number of eggNOG hits (transcript)	Number of KEGG hits (transcript)	Total number of unique GO terms (transcript)	Number of unique GO terms – Cellular Component (transcript)	Number of unique GO terms – Molecular Function (transcript)	Number of unique GO terms – Biological Process (transcript)
KingCrab16_MC	MC	40,941	56,911	1387	989	56,302,748	94.25	9358	6415	7729	8538	9928	1166	2300	6462
KingCrab16_YO2 Area #1, sample 2	unknown	55,435	78,090	1015	832	64,957,394	90.21	11,751	7524	8868	9802	10,663	1209	2454	7000
KingCrab16_YO3 Area #1, sample 3	unknown	58,899	82,295	1166	898	73,888,198	91.31	11,922	7527	8888	9588	10,808	1223	2498	7087
KingCrab20_MC	MC	39,106	53,921	1306	955	51,510,966	92.50	8905	6082	6918	7722	9614	1144	2255	6215
KingCrab20_YO1 Area #1	YO	77,081	111,353	1327	960	106,925,376	89.94	15,124	9407	12,368	13,486	11,989	1300	2840	7849
KingCrab20_YO2 Area #2	YO	76,992	111,341	1312	956	106,417,770	90.12	15,037	9423	12,322	13,409	12,020	1304	2841	7875
SnowCrab9_YOa	YO	57,079	97,557	1507	1015	99,003,920	89.05	16,149	9219	15,218	16,562	12,221	1295	2845	8081
SnowCrab9	YO, ESG	77,726	136,190	1491	1005	136,827,018	91.35	23,413	10,407	19,028	20,515	12,868	1369	2995	8504
KingCrab16	YO2, YO3, (i.e. unknown) ESG, HP, MC	150,154	226,560	1267	908	205,705,100	92.05	23,074	12,264	20,207	21,447	13,047	1387	3074	8586
KingCrab20	YO1, YO2, ESG, HP, MC	144,844	222,726	1407	962	214,241,763	91.94	13,516	12,453	21,055	22,508	13,123	1409	3093	8621
KingCrab16_20	YO, ESG, HP, MC	195,879	305,476	1278	904	276,268,985	91.65	27,536	13,360	24,871	26,451	13,320	1417	3139	8764

model (Le and Gascuel, 2008) was chosen for the Halloween genes, while the JTT (+G) model (Jones et al., 1992) was chosen for the CHH, MIH, ITP and ITP-like genes. For both trees a discrete Gamma (+G) distribution was used to model evolutionary rate differences among sites. For the Halloween genes, the rate variation model allowed for some sites to be evolutionarily invariable ([+I], 0.50% sites). The topology with superior log likelihood values were selected. Both the raw reads and the assemblies were deposited in the European Nucleotide Archive (ENA) under study accession number PRJEB44537.

2.5. Quantitative PCR (qPCR) analysis

qPCR was used to measure relative expression of regulatory genes involved in molting, growth and heat response in red king crabs kept at 4 °C or 10 °C as described in Section 2.1. Total RNA was extracted from the YO, ESG, claw muscle and hepatopancreas of the total of 24 crabs as described in Section 2.4. DNase treatment was performed using the TURBO DNAfree kit (Ambion) according to manufacturer's protocol. RNA quality and quantity were determined using NanoDrop 8000 (Thermo Scientific). 20 µl cDNA was synthesized using the High-Capacity RNA-to-cDNA kit (Thermo Fisher) according to manufacturer's protocol using 200 ng input of total RNA. Specific primers were designed using Primer Express 3 software (Life Technologies) for amplification of 17 target genes and 3 reference genes chosen from the generated transcriptomes (Supplementary Table S1). As reference genes we used the housekeeping genes β1 tubulin, elongation factor 2 (EF2), and ribosomal protein S5 (RPS5) (Fang et al., 2018; Jeon et al., 2020. The geometric mean of the three reference genes showed stable expression levels in the four tissues examined in both temperature groups. The amplification efficiency of each primer pair was calculated using eight 2-fold serial dilutions of a cDNA mix from all four organs according to the equation: $E = 10^{(-1/slope)}$ (Pfaffl, 2001). All primer pairs gave single distinctive melting peaks demonstrating that no primer dimers and unspecific amplification products were present. Absence of genomic DNA was verified by conducted qPCR in the absence of reverse transcriptase on three randomly selected RNA samples, and positive controls contained a cDNA mix from the four tissues. The qPCR was run in duplicates in 384 well plates using QuantStudio 5 (Thermo Fisher) using the following recommended parameters: Standard Run mode with 40 cycles at 50 °C for 2 min, 95 °C for 10 min and 60 °C for 1 min. Following by the melt curve stage at 95 °C for 15 s, 60 °C for 1 min and 95 °C for 15 s. Ct threshold was set at 0. 1. Each well contained Power SYBR Green PCR Master Mix, 300 nM final concentration of each primer, 7 µl diluted cDNA (1:40) and nuclease free water (Ambion) to a final reaction volume of 20 µl. All data were collected by the Quant Studio Design & Analysis Software (Thermo Fisher) and exported to Microsoft Excel for further analyses. The Pfaffl method was used to calculate relative expression (Pfaffl, 2001), and the geometric mean of the three reference genes was used to normalize the gene expression and remove non-biological variation (Vandesompele et al., 2002). Values from groups with lowest expression was used as calibrator as denoted by Pfaffl (2001).

2.6. Statistical analyses

Statistical analysis of gene expression was conducted in Microsoft Excel. Comparison between groups were performed using the unpaired Student's *t*-test. Values of $p < 0.05$ were considered significant.

3. Results

3.1. Identification of Y-organ

The YO of red king crab was localized ventrally near the basis of the mouth parts below an externally visible brown spot close to the urinary opening (Fig. 1A; see Tudge et al., 2012). The YO is a diffuse, anastomosing gland supported by connective tissue. As it was difficult to visually distinguish the YO from the surrounding tissue, three areas were sampled for histological analysis (Fig. 1B). The YO cells were characterized by high nuclear density that was easily distinguished from the low nuclear density of the surrounding connective tissue in samples taken from Areas 1 and 2, whereas Area 3 did not contain YO tissue (Fig. 1C-F). Consequently, YO tissue from areas #1 and #2 were used from RNA sequencing. In contrast, the YO of snow crab was identified as an ellipsoid, compact white gland clearly distinguishable from the surrounding connective tissue.

3.2. Sequence data and de novo transcriptome assemblies

Eleven *de novo* transcriptome assemblies were generated from YO, ESG, hepatopancreas and claw muscle of two individuals of red king crab and from YO and ESG of one snow crab in intermolt (Table 1). For red king crab, we generated separate assemblies of claw muscle and putative YO tissues, as well as assemblies that contained all reads from all the tissues of one individual. Furthermore, reads of both individuals were combined to a comprehensive assembly. For snow crab, one assembly which contained reads from YO only and one from YO and ESG combined were generated. The total number of assembled bases ranged from 51,510,966 in king crab muscle to 276,268,985 in the comprehensive king crab assembly (Table 1). The number of Trinity "genes" was in the range 39,106–195,879 and from 53,921 to 305,476 contiguous sequences in total. The mean lengths of the transcripts were in the range 832–1015 bp with their median in the range 1015–1507 bp. The contig lengths were similar to those obtained in previous studies (Das and Mykles, 2016; Hall et al., 2020). About 90–94% of the reads mapped back to the transcriptomes using Bowtie. Completeness of Benchmarking Universal Single-Copy Orthologs (BUSCOs) ranged from 64% in the assembly KingCrab16_YO3 to 98% in the comprehensive king crab assembly compared to the Arthropoda_odb9 (1066 BUSCOs) lineage dataset. BLASTx against NCBI non-redundant database and UniProt/Swissprot database resulted in up to 27,536 and 13,360 annotated genes, respectively. 13,320 unique Gene Ontology (GO) terms were identified in the comprehensive king crab assembly, which divide into 1417 terms in the category Cellular Component, 3139 terms in Molecular Function and 8764 terms in Biological Process. Figures tended to be higher than in the study by Stillman et al. (2020, e.g. 18,049 BLASTx hits and 8356 unique GO terms in the Larval transcriptome for comparison), except in contig length, which may be due to different sequencing, assembly and analysis methods. This, too, suggests that genes were represented well, despite focusing on a set of tissue types rather than including whole organisms as in Stillman et al. (2020). When broad eggNOG terms were considered, the number of assignments in muscle and YO tissues were similar (Fig. 2A). Cluster analysis of KEGG proteins grouped king crab YO and muscle tissue samples, respectively, and identified YO of snow crab as an outgroup (Fig. 2B).

3.3. Identification of multiple molt-, growth- and stress-related factors

The identity of the red king crab YO was confirmed by the identification of the Halloween gene transcripts *spook*, *phantom*, *disembodied, shadow* and *shade-like*, together with *neverland* (Supplementary Table S2), which are the first ecdysteroidogenic enzymes described in anomurans. The predicted red king crab enzymes shared high similarity with the brachyuran orthologs, except for Shade-like, which did not cluster with decapod Shed, but branched off from the adjacent Disembodied and non-decapod Shade clades in the phylogenetic tree (Fig. 3). Snow crab YO contained two different *shed* transcripts most similar to *shed4* and *shed5*, in addition to *spook*, *phantom*, *disembodied*, *shadow* and *neverland*. The major ecdysone response gene *Broad-Complex* (*Br-C*) and the *CYP18A1* gene encoding the enzyme catalyzing 20-HE degradation were also identified in both species.

Several CHH family members, which are characterized by six

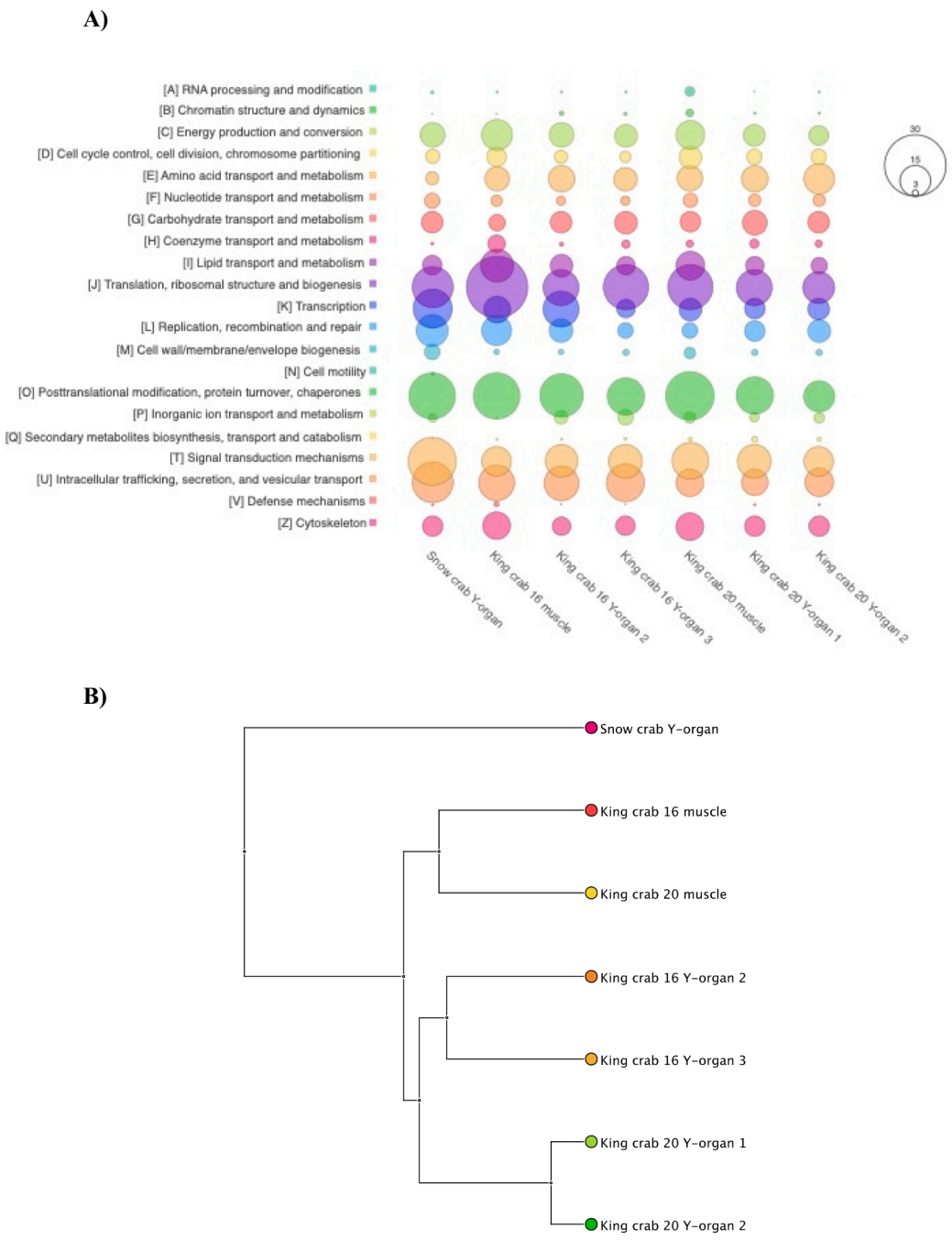

Fig. 2. Comparison of Y-organ and claw muscle annotated transcriptome assemblies of red king crab and snow crab. A) EggNOG contiguous read assignments to the respective categories in snow crab Y-organ and king crab Y-organ and claw muscle. The number of unclassified contigs is not shown. B) UPGMA tree based on the number of contigs assigned to KEGG terms on enzyme level of samples of snow crab YO, king crab 16 YO2, YO3 and claw muscle and king crab 20 YO1, YO2 and claw muscle using the Bray-Curtis method. Note that it is unlikely that putative YO samples of king crab 16 were Y-organ tissue due to the absence of Halloween genes (Supplementary Table S1). King crab 16 and 20 were in premolt and late premolt, respectively, while snow crab 9 was in intermolt. (For interpretation of the references to colour in this figure legend, the reader is referred to the web version of this article.)

conserved cysteines, were identified in the red king crab and snow crab transcriptomes. MIH has a glycine residue inserted close to the first cysteine and is lacking a precursor related peptide (PRP) preceding the mature hormone in CHH and non-decapod ITP (Fig. 4A). Red king crab was found to express a single CHH and two highly similar MIH isoforms, in addition to an ion-transport peptide (ITP)-like member. Snow crab ESG contained transcripts encoding single MIH and CHH, which is identical to the recently identified CHH1 isoform (KAG0710697) but showed low similarity with the CHH2 isoform (AHM93480.1, Chung et al., 2014) (Fig. 4A). Red king crab CHH is highly similar to hermit crab CHH (86% identity), but both shared only 56% identity with the squat lobster CHH. Alignment of the three anomurans with the brachyuran mature CHH revealed four positions that distinguish the two groups, but showed conservation of the functionally critical N-terminal dibasic cleavage site, the three disulfide bridges and the C-terminal amidation signal Val-Gly-Lys (Supplementary Fig. S1). The anomuran and brachyuran CHH consistently clustered in the phylogenetic tree, except for snow crab CHH1 (Fig. 4B). Red king crab ITP-like and the brachyuran orthologs formed a clade separate from the insect ITPs and the crustacean MIH clades.

The transcriptomes included a variety of other peptide hormones and neuromodulators, such as red pigment concentrating hormone (RPCH), pigment dispersing hormone (PDH), crustacean cardioactive peptide (CCAP), somatostatin, myostatin, follistatin, allatostatin and cystatin. Growth-related factors in the mTOR signaling pathway comprised mTOR, AMPKα, Rheb, AKT, raptor (regulatory associated protein of mTOR) and rictor (rapamycin-insensitive companion of mTOR) (Supplementary Table S4).

Both red king and snow crab expressed several molt-related nuclear receptors, including EcR, RXR, E75, HR3 and FTZ-F1 (Supplementary

Table S4). The three EcR isoforms expressed in red king crab are likely coded by two genes designated *EcR1* and *EcR2*, while the alternative splice variant EcR3 differs from the EcR1 form in the N-terminal end and in the hinge domain linking the conserved DNA-binding and ligand-binding domains. Various photoreceptors are probably of importance for performing seasonal spawning migrations from large depths to shallow water, and the repertoire of opsins included rhodopsin, melanopsin, peropsin and parapinopsin (Supplementary Table S4). The crustacean nervous system uses various excitatory and inhibitory neurotransmitters (Cao et al., 2019) and receptors for glutamate, acetylcholine, histamine, dopamine, GABA and serotonin (5-HT) are expressed in red king crab and snow crab (Supplementary Table S4).

Among the many stress-response genes expressed by the two crab species, we identified multiple high- and low-molecular HSPs, heat shock factor 1 (HSF-1), hypoxia inducible factor 1 (HIF1) α and β subunits, HIF1α inhibitor (HIF1AN), HIF-prolyl hydroxylase and hypoxia up-regulated protein 1 (HYOU1). Both species also possessed cold-shock proteins, which are RNA/DNA binding proteins playing a significant role in cold acclimation (Lindquist and Mertens, 2018) (Supplementary Table S4).

3.4. Molecular responses of red king crab to elevated temperature

We examined effects of elevated temperature on the expression of key genes involved in molting, growth and heat shock response in male red king crabs kept at either 4 °C or 10 °C for two weeks. The Halloween genes were mainly expressed in YO and tended to be upregulated at the higher temperature, but significant differences were only found between crabs after 4 °C acclimation and after two weeks at 10 °C (Fig. 5A). These groups also differed significantly in the *EcR* mRNA levels in YO with higher levels at 10 °C. A similar trend was shown in claw muscle after two weeks at 4 °C or 10 °C, while the gene expression of the receptor in hepatopancreas were significantly lower at 10 °C than at 4 °C (Fig. 5B). The ESG contained about 6-fold higher transcript levels of CHH than MIH, and both tended to be upregulated at high temperature, but the difference was not significant (Fig. 5C).

The expression of the four mTOR pathway genes was influenced by temperature, but the effect differed between the organs examined. *mTOR* was significantly upregulated at high temperature in YO and in claw muscle, which also showed a similar trend for *AMPKα* and *AKT* (Fig. 6). These expression patterns contrasted with the significantly lower mRNA levels of *Rheb* and *AMPKα* in the hepatopancreas of crabs kept for two weeks at 10 °C than those at 4 °C, but low *Rheb* levels were also measured after the initial 4 °C acclimation. The expression of the four genes showed no significant changes in ESG during the experiment.

We examined the response of the adult crabs to chronic temperature changes by quantifying the expression levels of *hsp90a, hsp90b*, *hsp70* and *hsp60* (Fig. 7). *hsp90b* and *hsp70b* were the major transcripts in the four tissues examined, except from the high *hsp90a* levels in claw muscle. The *hsp90b*, *hsp70* and *hsp60* mRNA levels in hepatopancreas were significantly lower after two weeks at 10 °C than at 4 °C (Fig. 7A), and the *hsp90b* transcript showed about half the levels at high temperature also in claw muscle and YO (Fig. 7B and D). The expression of *hsp70* was also significantly downregulated in ESG at high temperature

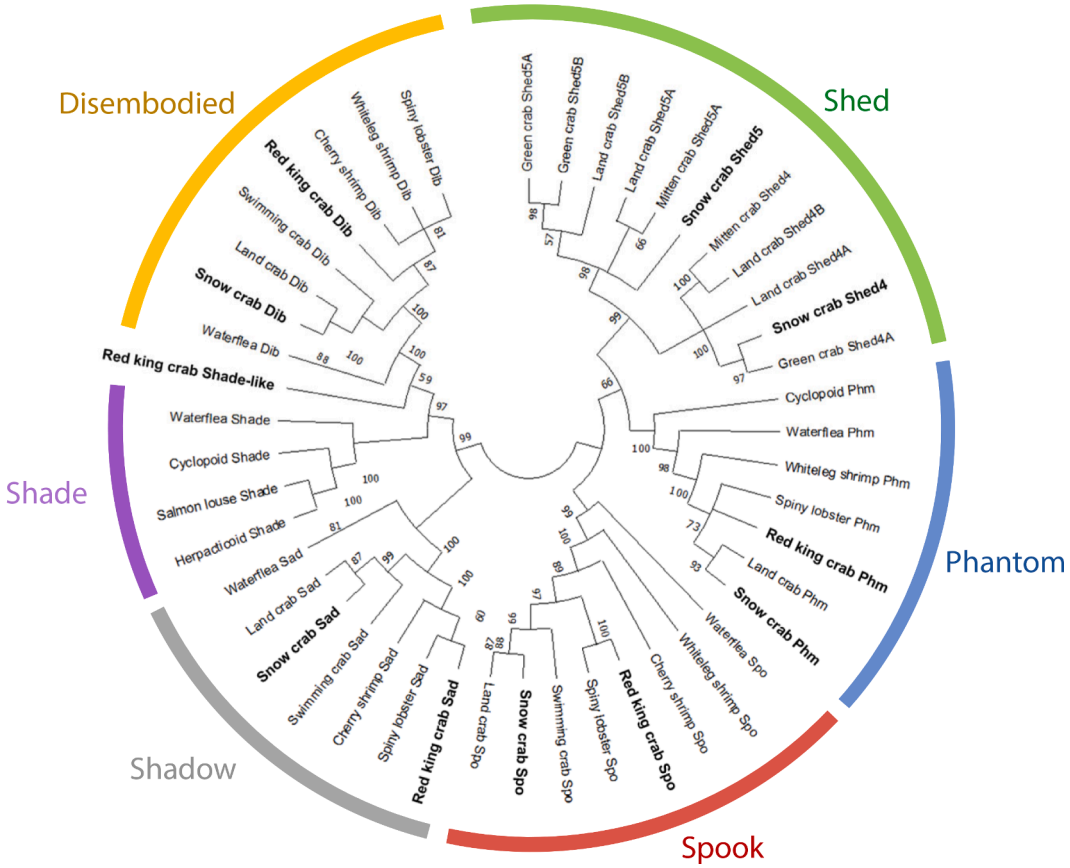

Fig. 3. Phylogenetic relationship of the Halloween genes from various crustacean species, including red king crab and snow crab. The tree was generated based on 46 whole amino acid sequences aligned by MUSCLE and there was a total of 698 positions in the final dataset. The analyses were conducted in MegaX using the Maximum likelihood method based on the LG (+G + I) model. To assess the tree topological stability 100 bootstrap resamplings were made. All branches with less than 50 bootstrap confidence value were collapsed. Accession numbers are listed in Supplementary Table S3. (For interpretation of the references to colour in this figure legend, the reader is referred to the web version of this article.)

```
KingCrab CHH          PRP KRQAF-DRSCQGVY-DRGLFKKLERVCDDCYNLYRKPYVEVGCKANCYANKIFRQCISELLLEDVMEEYRDAIQMVGK
HermitCrab CHH       PRP KRQAF-DRSCKGVY-DRGLFKKLERVCDDCYNLYRKPYVEVGCKANCYANSIFRQCIGDLLLEDVVEEYAQAIQMVGK
SquatLobster CHH      PRP KRQAF-DRNCKGVY-DRGIFQKLEQVCDDCYNLYRKPYVAVSCKSNCYANDVFRQCLTELLLEDVLGEYARAVQSVGK
SnowCrab CHH1         PRP KRSAYVDSSCQGLY-SRRVWDDLAYVCEDCANVFRKDGFQAKCRKGCFASDTFAHCLIVLDKDVNVYQAMATSLRGS
SnowCrab CHH2         PRP KRQVY-DTSCKGMY-DRGLFSDLEHVCDDCYNLYRNPHVATACRGNCYSNLVFRQCMEDLLLMEEFDKYARAIQTVGKKK
KingCrab MIH1             GDSWHSIYECPGLMGNRHIYDKVVRVCDDCYNIYRSTDIAVRCRSNCFLNDEFKTCLRANERYDELHDFQRWISILSAGRK
KingCrab MIH2             GDSWHNIYECPGLVGNRNIYDKVVRVCDDCYNIYRSTDIAVRCRSNCFQNDEFKNCLRVNERYDELHDFQRWISILRAGRK
SnowCrab MIH              TAAMNINKDCRNVYGNRYIYEEVEWICDDCSNIFRKGNIGSKCRRNCFNNTDFEWCVDRTMRSTDLQQLREYVRILNYGRDWIV
KingCrab ITP-like         YTQREFKQYCNGEY-DRHAYSELSDVCYECRNLFRNNHVLYDCKDNCFNSRMFGICVDALALSPKLEVFDRHRMLLSGEPTSEE
AntShrimp ITP-like        TYKEFQYINCQGRF-DKEQYASLTNICEDCHNVYRNPDVLLGCKADCFRNSLFPKCVSMLLLDQREPELSKMVYTVSGKR
Waterflea ITP         PRP KRS-FFDINCKGLY-DKSIFARLDRICQDCYNLYREPELHTLCRSECFTTPFFKACLKVLLLEDQDPDYSEMIDKIGR
```

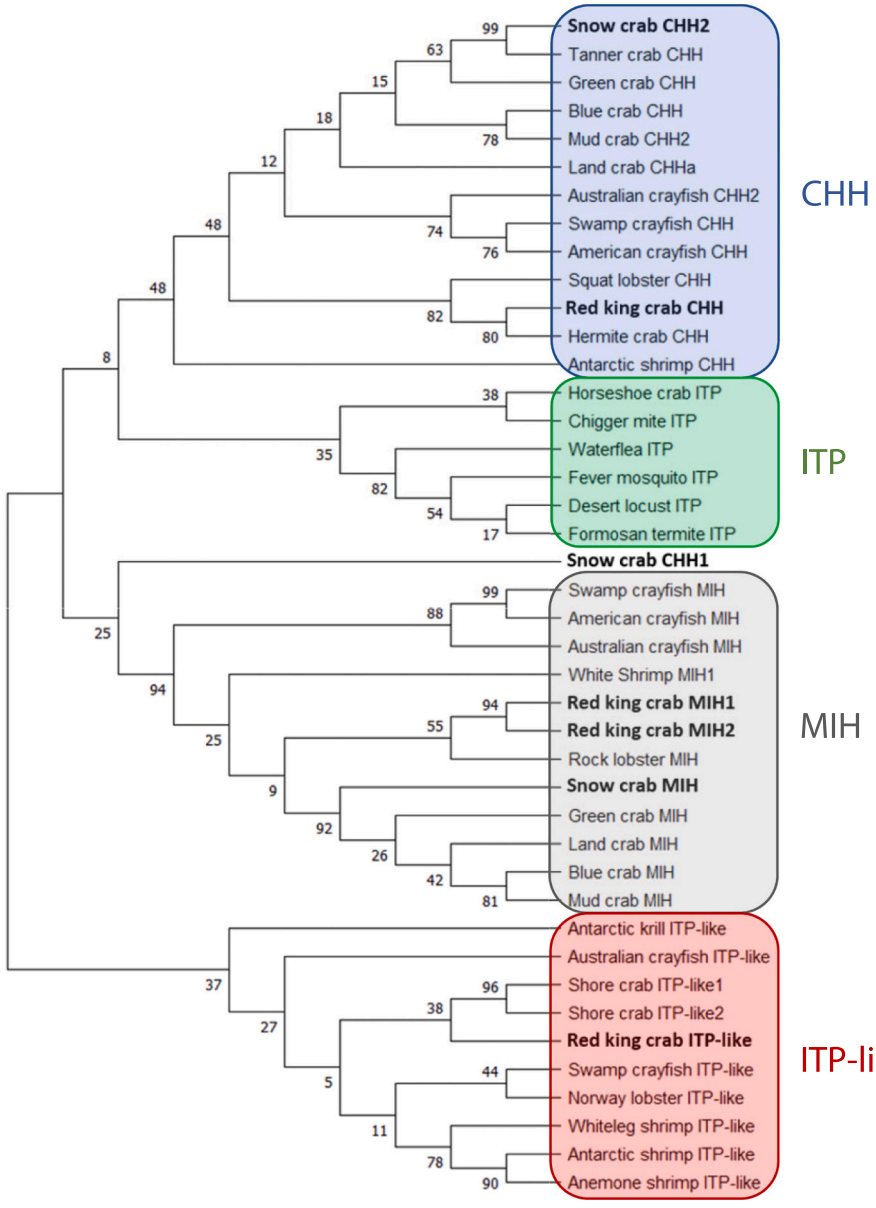

Fig. 4. Phylogenetic analysis of CHH family members in red king crab and snow crab. A. Sequence alignment of CHH, MIH and ITP-like from red king crab and snow crab together with hermit crab CHH, squat lobster CHH, Antarctic shrimp ITP-like and waterflea ITP. The six conserved cysteines are colored (yellow), and the PRP region (boxed) and dibasic cleavage site (grey) preceding the mature CHH and ITP are indicated. Predicted C-terminal processing, including putative amide donor Gly (underlined), and the Gly residue (grey) inserted in MIH are also shown. B. Phylogenetic relationship of CHH, MIH, ITP and ITP-like from various crustaceans, including red king crab and snow crab. The tree was generated based on 42 amino acid sequences aligned by MUSCLE and there was a total of 119 positions in the final dataset. The analyses were conducted in MegaX using the Maximum likelihood method based on the JTT (+G) model. To assess the tree topological stability 100 bootstrap resamplings were made. No branches were collapsed. Accession numbers are listed in Supplementary Table S3. (For interpretation of the references to colour in this figure legend, the reader is referred to the web version of this article.)

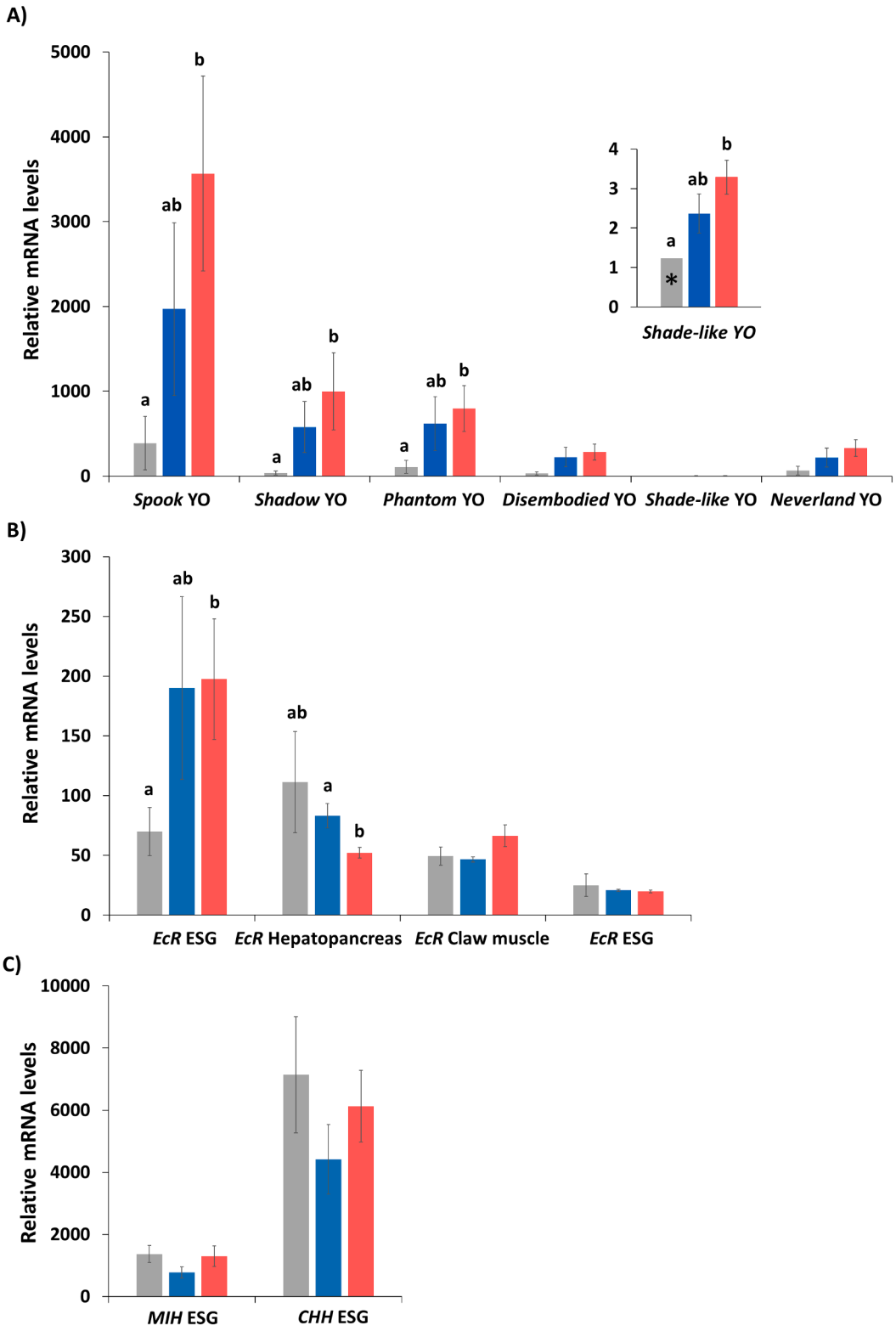

Fig. 5. Relative mRNA levels of molt- related genes in adult red king crab measured after 4 °C acclimation (grey) and after two additional weeks at 4 °C (blue) or 10 °C (red) ($n = 8$). A) Expression of *spook, shadow, phantom, disembodied, shade-like* and *neverland* in YO. B) Ecdysteroid receptor (*EcR*) expression in ESG, YO, hepatopancreas and claw muscle. C) Expression of *MIH* and *CHH* in ESG. The results were calibrated to the mean expression of *shade*-like in YO at T0 4 °C indicated by an asterisk (*) in A. All data is shown as mean ± SEM and statistical differences (multiple unpaired *t*-tests, $p < 0.05$) between temperatures for the respective genes are indicated by different letters. (For interpretation of the references to colour in this figure legend, the reader is referred to the web version of this article.)

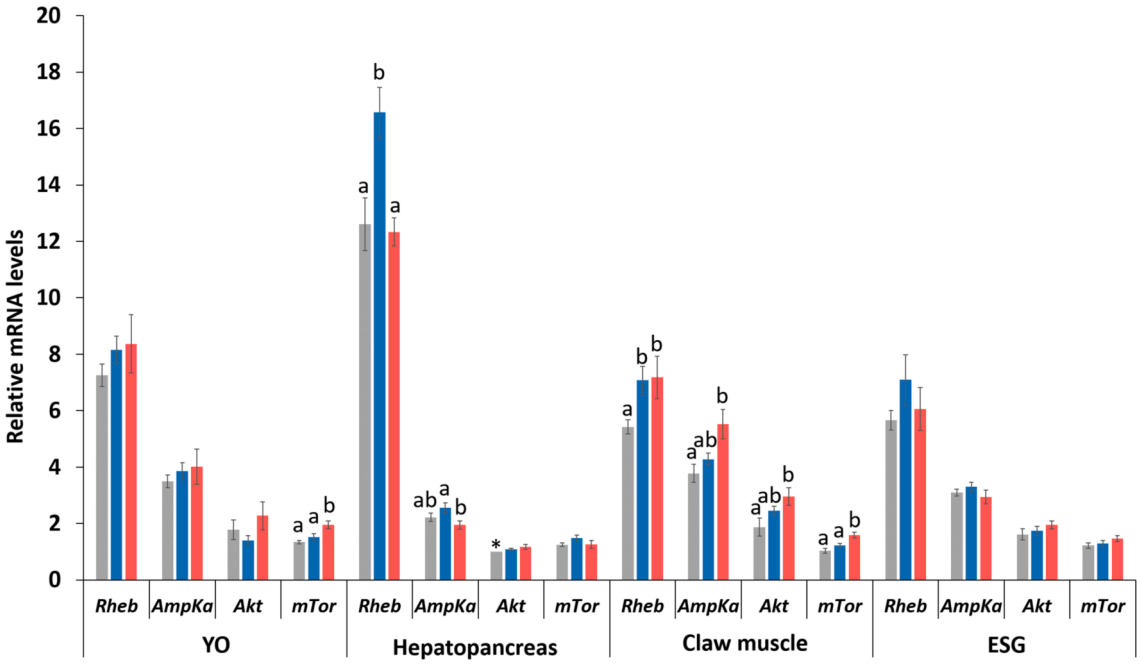

Fig. 6. Tissue expression of *Rheb, AMPKα, AKT* and *mTOR* in adult red king crab after 4 °C acclimation (grey) and after two additional weeks at 4 °C (blue) or 10 °C (red). The mRNA levels were qPCR quantified in YO, hepatopancreas, claw muscle and ESG (n = 8). The results were calibrated to the mean expression of *Akt* in hepatopancreas at acclimation (*). All data is shown as mean ± SEM and statistical differences (multiple unpaired *t*-tests, $p < 0.05$) between temperatures for the respective genes are indicated by different letters. (For interpretation of the references to colour in this figure legend, the reader is referred to the web version of this article.)

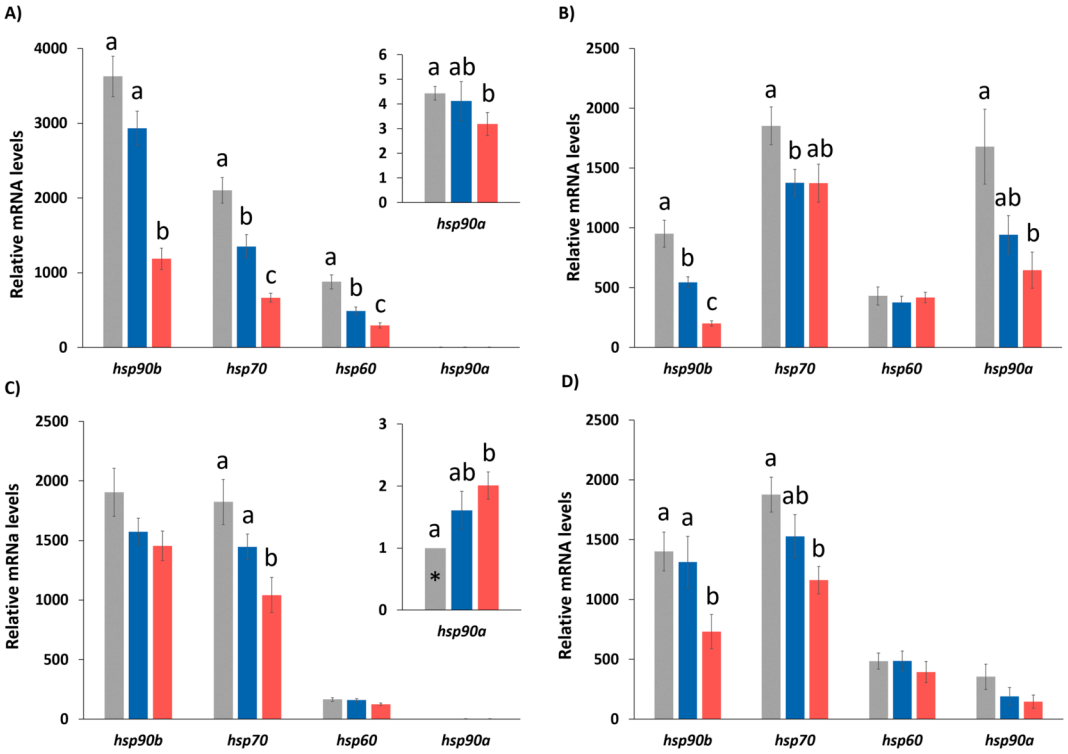

Fig. 7. Tissue expression of *hsp90b*, *hsp70*, *hsp60* and *hsp90a* in adult red king crab after 4 °C acclimation (grey) and after two additional weeks at 4 °C (blue) or 10 °C (red) (n = 8). The mRNA levels were qPCR quantified in A) hepatopancreas, B) claw muscle, C) ESG, D) YO. The results were calibrated to the mean expression of *hsp90a* in ESG at T0 4 °C indicated by an asterisk (*). All data is shown as mean ± SEM and statistical differences (multiple unpaired *t*-tests, $p < 0.05$) between temperatures for the respective genes are indicated by different letters. Note the different scaling of the y-axis in A. (For interpretation of the references to colour in this figure legend, the reader is referred to the web version of this article.)

(Fig. 7C). It should be noted that the expression of the four *hsp* genes in at least one of the tissues examined was significantly higher after 4 °C acclimation than after additional two weeks at 4 °C or at 10 °C.

4. Discussion

This study describes for the first time the ecdysteroid biosynthetic enzymes in anomuran crabs by *de novo* transcriptome analysis of four organs, including the YO, in red king crab. The YO shows a variety of anatomic features in crustaceans and forms an elongated structure situated on a cuticular outgrowth of the mandibles in the anomuran crab *Anapagurus hyndmanni*, while the common hermit crab (*Pagurus bernhardus*) and long-clawed porcelain crab (*Pisidia longicornis*) have a tubular and globular YO, respectively (Lachaise et al., 1993). The crucial role played by the Halloween genes in the regulation of the molt cycle is corroborated by the well conserved sequences in red king crab, except for the Shade-like protein. Insect Shade is used by various non-decapods, such as water flea and salmon louse, for catalyzing the conversion of ecdysone to the active molting hormone 20- hydroxyecdysone (20E) (Mykles, 2011; Ventura et al., 2017; Swall et al., 2021), which is the main hormone also in the red king crab hemolymph (Dvoretsky and Dvoretsky, 2010). The ecdysone 20-mono-oxygenase enzyme has recently been found to be expressed by multiple *shed* genes in several decapod species, including spiny lobster and blackback land crab (Ventura et al., 2017, 2018; Swall et al., 2021). The snow crab genome has five *shed* genes (NCBI accession PRJNA602365) of which the two *shed* transcripts identified in this study share only 50% identity. This is consistent with the relatively low homology between the Shed paralogs in blackback land crab (Swall et al., 2021). The presence of a Shade-like protein in red king crab suggests that Shade was retained in anomurans after the separation from brachyuran crabs (Wolfe et al., 2019), whereas brachyurans possess multiple Shed paralogs probably resulting from gene duplications.

King crabs (Lithodidae) are thought to have originated from the asymmetric hermit crabs (Paguridae) and later transformed to a crab-like crustacean with the pleon folded underneath the compact cephalothorax according to the so-called “hermit to king” hypothesis (Cunningham et al., 1992). The close phylogenetic relationship between lithodid and pagurid crabs is supported by the asymmetric pleon of king crabs (Keiler et al., 2013) and the high similarity of ribosomal nuclear sequence data and mitogenomes of red king crab and hermit crab, which differ considerably from the mitogenome of the anomuran squat lobster (Kim et al., 2013; Noever and Glenner, 2018). Consistently, the nuclear DNA-coded protein CHH shows high similarity in red king crab and hermit crab, while they share low similarity with squat lobster CHH. The few functional analyses of crustacean CHH mutants includes the Glu54Ala substitution in mud crab CHH that did not reduce the hyperglycemic activity (Liu et al., 2015). This corresponds to one of the four substituted positions identified in anomuran CHH and suggests conserved functions, but the pleiotropic activities displayed by the brachyuran CHH (Chen et al., 2020) should be further investigated in anomurans. Earlier attempts to isolate MIH from hermit crab and squat lobster failed, but distinct CHH- and MIH-immunoreactive perikarya were localized in the hermit crab ESG (Montagné et al., 2008). In addition to these Type-I and -II peptides, respectively, red king crab also expressed the Type-III ITP-like peptide, which has been reported in several malacostracan species (Manfrin et al., 2015; Toullec et al., 2017). The function of crustacean ITP-like is unknown, while a possible ecdysis-related function has been suggested for insect ITP, in addition to regulating water homeostasis (Dircksen, 2009).

Recent transcriptome analyses of the crustacean YO and ESG have revealed complex gene regulatory networks underlying the conserved signaling pathways of molting and growth (Gao et al., 2015; Das and Mykles, 2016; Oliphant et al., 2018; Shyamal et al., 2018; Su et al., 2020). The complexity seems to be increased by the influences of environmental factors, particularly temperature, on the gene expression of key regulators. Shortened molt intervals in juvenile mud crabs (*Scylla paramamosain*) at elevated temperature were associated with increased *EcR* expression (Gong et al., 2015), and temperature compensation of the expression of *MIH*, *CHH* and mTOR signaling genes in temperate juvenile Dungeness crabs (*Metacarcinus magister*) contributed to regulate molting in the 10 °C to 20 °C range (Wittmann et al., 2018). Involvement of the Halloween genes in the thermal response of crustaceans was suggested by the up- or downregulated expression of various P450 genes, including *spook*, *phantom* and *shade*, in the alligatorweed flea beetle (*Agasicles hygrophila*) acutely exposed to high temperature (Zhang et al., 2018). Red king crabs showed a tendency towards upregulation of the Halloween and *EcR* genes in the YO at elevated temperature, but large individual variations were measured that may be explained by the challenges in the dissection of the diffuse organ. These patterns of gene expression may relate to temperature-dependent acceleration of the molt cycle. In the land crab *Gecarcinus lateralis* Halloween gene and *EcR* expression increase from postmolt to intermolt and from intermolt to premolt (Benrabaa, 2019). It is likely that this is a continuous process, which could, at least in part, explain our results. The *MIH* and *CHH* mRNA levels in ESG were not affected by temperature in our study, but *MIH* was downregulated in Dungeness crab ESG at high temperature (Wittmann et al., 2018). Our results are in line with previous findings suggesting that hemolymph MIH and CHH levels are regulated on a different level of organization, i.e. protein translation and secretion (Mykles and Chang, 2020).

Tissue-specific differences became evident when high resolution analyses were employed, e.g. on KEGG enzyme level (compare Fig. 2A and B, Robalino et al., 2007), and when specific sets of genes were considered (Supplementary Table S2, Covi et al., 2010; MacLea et al., 2012; Wittmann et al., 2018). Swamp crayfish (*Procambarus clarkii*) showed tissue-specific responses to eyestalk ablation by increased *EcR* and *RXR* mRNA levels in muscle and ovaries, but downregulated receptor expression in hepatopancreas, indicating that different tissues play different roles and coordinate their functions in molting (Dai et al., 2016). Here, red king crab responded to high temperature by an upregulated trend in *EcR* expression in YO and claw muscle, while decreased *EcR* mRNA levels were found in hepatopancreas. The mTOR signaling genes also suggested temperature-related differences in tissue expression of which *AMPKα* and *AKT* tended to be upregulated in claw muscle at high temperature, while *AMPKα* and *Rheb* were downregulated in hepatopancreas. Tissue-specific responses to temperature were also observed in juvenile Dungeness crabs, which displayed the most pronounced differences in cardiac expression of *Rheb* between 10 °C and 15 °C, with no further downregulation at exposure to 20 °C after two weeks of acclimation (Wittmann et al., 2018). This indicates that protein turnover is maintained and assures the structure and function of the claw muscle and heart muscle at high temperature. Conversely, the higher expression of *Rheb* and *AMPKα* in the hepatopancreas of red king crab at 4 °C compared to 10 °C is consistent with the upregulation of genes involved in protein synthesis and degradation in the liver of the cold-eurythermal eelpout (*Pachycara brachycephalum*) at chronic exposure to low temperature (Windisch et al., 2011). This may reflect efficient food conversion in the cold during long-term experiments (Siikavuopio and James, 2015; Windisch et al., 2014). The deep-water living adults and the shallow-water juveniles of red king crab may differ in temperature tolerance and changes in cellular energy allocation (Stiansen et al., 2009; Stoner et al., 2010; Long and Daly, 2017), which may relate to the expression of genes involved. Juveniles kept at either 10.5, 12.5 or 14.5 °C for 20 days showed strong effects of acclimation on transcriptome level. Temperature mainly affected transcripts involved in cuticle formation and regulation, but did not affect any genes of the mTOR pathway (Stillman et al., 2020). However, changes smaller than 2-fold were excluded from their analysis, and tissue-specific responses may have equaled out in this whole organism study.

The thermal habitat of red king crab in the Barents Sea spans ambient temperatures from −0.8 to 8.5 °C with males predominantly at 4–6 °C

and females at 5–7 °C (Pinchukov and Sundet, 2011). Even though 10 °C is beyond the temperature wild adult red king crabs experience, except during spawning migration, this may not be a temperature that causes cellular thermal stress affecting the folding of proteins at the time scale of our study. This may explain why the crabs exposed to 10 °C for two weeks showed either lower or no changes in the expression of the four *hsp* genes examined, except for the increased *hsp90a* levels in ESG. In contrast to HSP90a, HSP90b is thought to be constitutive, but can also be induced and is probably involved in long-term cellular adaptation (Sreedhar et al., 2004). The duration and magnitude of heat stress influence the dynamics of *hsp* gene expression (Buckley and Hofmann, 2004; Logan and Buckley, 2015), and the upregulation of HSPs in the eurythermal goby fish *Gillichthys mirabilis* in response to acute thermal stress was not observed after four weeks acclimation to high temperature (Logan and Somero, 2010). Downregulated *hsp* levels may also result from the faster turnover of the mRNAs than the turnover of the proteins itself (Buckley et al., 2006). Reduced mRNA levels after thermal acclimation may thus reflect the completion of the induced synthesis of the chaperones and may result in the cessation of a cellular stress response. Nevertheless, maintenance costs for homeostasis at elevated temperatures may be high and result in a trade-off between energy allocation to homeostasis and less energy available for growth and reproduction (Hochachka and Somero, 2002; Sokolova et al., 2012; Logan and Buckley, 2015). The heat shock response varies among organisms that occupy different thermal environments, and contrasting with eurythermal intertidal species, such as the porcelain crab (*Petrolisthes cinctipes*), stenothermal organisms like Antarctic notothenioid fish and the gammarid crustacean *Paraceradocus gibber* do not respond to thermal stress with increased HSP synthesis (Clark and Peck, 2009; Shin et al., 2014; Garland et al., 2015). Intertidal snails reduced HSP protein levels at moderate temperature increase and showed elevated levels only after long-term exposure to infrequently experienced high field temperatures (Tomanek and Somero, 1999, 2002). These studies also showed that animals exposed to constant temperatures in the laboratory exhibit lower HSP protein levels than animals sampled from the field. This resembles our observation of higher *hsp* mRNA levels in crabs sampled after acclimation at the more variable ambient temperature. The multiple temperature sensitive genes identified in juvenile red king crabs exposed to elevated temperatures comprised different clusters displaying upregulated or downregulated expression patterns dependent on the pH conditions (Stillman et al., 2020). Three contigs annotated as HSP83 only showed small and variable responses to temperature (cluster 7 in Stillman et al., 2020). While we show that constitutive and heat-inducible HSPs are expressed in a temperature-dependent and tissue-specific manner in response to acclimation, further studies should address the potential for acclimation on additional organismal levels of organization, and also the acute heat shock response in the cold-eurythermal red king crab.

5. Conclusions

Multiple expressed genes involved in various physiological functions were identified in *de novo* transcriptome assemblies from the sub-Arctic red king crab and snow crab. The phylogenetic analyses of the CHH family and Halloween genes support the phylogenetic relation between the anomuran and brachyuran crabs. Genes playing key roles in molting and growth tended to be upregulated in adult red king crab at elevated temperature, while several *hsp* genes were downregulated. The tissue- and gene-specific responses reflect regulatory processes on molecular level during acclimation of this cold-eurythermal species. The transcriptome data provides a valuable resource for comparative studies of adaptive traits, such as cold hardiness and dim light vision, in the two distant sub-Arctic crabs.

Supplementary data to this article can be found online at https://doi.org/10.1016/j.cbpb.2021.110678.

Declaration of Competing Interest

The authors declare that they have no known competing financial interests or personal relationships that could have appeared to influence the work reported in this paper.

Acknowledgments

This is a contribution to the PACES II research program (WP 1.6) of the Alfred Wegener Institute, Helmholtz Center for Polar and Marine Research, funded by the Helmholtz Association, Germany. This work was partly supported by the Research Council of Norway, project no. 281053).

References

Anger, K., Thatje, S., Lovrich, G., Calcagno, J., 2003. Larval and early juvenile development of *Paralomis granulosa* reared at different temperatures: tolerance of cold and food limitation in a lithodid crab from high latitudes. Mar. Ecol. Prog. Ser. 253, 243–251.

Benrabaa, S.A.A.S., 2019. Regulation of Halloween Genes and Ecdysteroid Responsive Genes in Molting Gland of Blackback Land Crab *Gecarcinus lateralis* by Molt-inhibiting Hormone, mTOR and TGFβ Signaling Pathways. Colorado State University, ProQuest Dissertations Publishing (13814559).

Buckley, B.A., Hofmann, G.E., 2004. Magnitude and duration of thermal stress determine kinetics of hsp gene regulation in the goby *Gillichthys mirabilis*. Physiol. Biochem. Zool. 77, 570–581.

Buckley, B.A., Gracey, A.Y., Somero, G.N., 2006. The cellular response to heat stress in the goby *Gillichthys mirabilis*: a cDNA microarray and protein-level analysis. J. Exp. Biol. 209, 2660–2677.

Bushnell, B., 2015. BBMap Short Read Aligner, and Other Bioinformatic Tools. Available online at. http://sourceforge.net/projects/bbmap.

Cao, Q., Wang, Y., Chen, B., Ma, F., Hao, L., Li, G., Ouyang, C., Li, L., 2019. Visualization and identification of neurotransmitters in crustacean brain via multifaceted mass spectrometric approaches. ACS Chem. Neurosci. 10, 1222–1229.

Chen, H.Y., Toullec, J.Y., Lee, C.Y., 2020. The crustacean hyperglycemic hormone superfamily: progress made in the past decade. Front. Endocrinol. 11, 578958.

Christiansen, J.S., Sparboe, M., Sæther, B.S., Siikavuopio, S.I., 2015. Thermal behaviour and the prospect spread of an invasive benthic top predator onto the Euro-Arctic shelves. Divers. Distrib. 21, 1004–1013.

Chung, A.C., Durica, D.S., Clifton, S.W., Roe, B.A., Hopkins, P.M., 1998. Cloning of crustacean ecdysteroid receptor and retinoid-X receptor gene homologs and elevation of retinoid-X receptor mRNA by retinoic acid. Mol. Cell. Endocrinol. 139, 209–227.

Chung, J.S., Ahn, I.S., Yu, O.H., Kim, D.S., 2014. Crustacean hyperglycemic hormones of two cold water crab species, *Chionoecetes opilio* and *C. japonicus*: isolation of cDNA sequences and localization of CHH neuropeptide in eyestalk ganglia. Gen. Comp. Endocrinol. 214, 177–185.

Clark, M.S., Peck, L.S., 2009. HSP70 heat shock proteins and environmental stress in Antarctic marine organisms: a mini-review. Mar. Genom. 2, 11–18.

Covi, J.A., Bader, B.D., Chang, E.S., Mykles, D.L., 2010. Molt cycle regulation of protein synthesis in skeletal muscle of the blackback land crab, *Gecarcinus lateralis*, and the differential expression of a myostatin-like factor during atrophy induced by molting or unweighting. J. Exp. Biol. 213, 172–183.

Cunningham, C.W., Blackstone, N.W., Buss, L.W., 1992. Evolution of king crabs from hermit crab ancestors. Nature 355, 539–542.

Dai, T.H., Sserwadda, A., Song, K., Zang, Y.N., Shen, H.S., 2016. Cloning and expression of ecdysone receptor and retinoid X receptor from *Procambarus clarkii*: induction by eyestalk ablation. Int. J. Mol. Sci. 17, 1739.

Das, S., Mykles, D.L., 2016. A comparison of resources for the annotation of a *de novo* assembled transcriptome in the molting gland (Y-organ) of the blackback land crab, *Gecarcinus lateralis*. Integr. Comp. Biol. 56, 1103–1112.

Das, S., Vraspir, L., Zhou, W., Durica, D.S., Mykles, D.L., 2018. Transcriptomic analysis of differentially expressed genes in the molting gland (Y-organ) of the blackback land crab, *Gecarcinus lateralis*, during molt-cycle stage transitions. Comp. Biochem. Physiol. 28D, 37–53.

Dawe, E.G., Colbourne, E.B., 2002. Distribution and demography of snow crab (*Chionoecetes opilio*) males on the Newfoundland and Labrador Shelf. In: Paul, A.J., Dawe, E.G., Elner, E., Jamieson, G.S., Kruse, G.H., Otto, R.S., Sainte-Marie, B., Shirley, T.C., Woodby, D. (Eds.), Crabs in Cold Water Regions: Biology, Management and Economics. Alaska Sea Grant College Program, University of Alaska Fairbanks, pp. 577–594.

DeLeo, D.M., Pérez-Moreno, J.L., Vásquez-Miranda, H., Bracken-Grissom, H.D., 2018. RNA profile diversity across arthropoda: guidelines, methodological artifacts, and expected outcomes. Biol. Meth. Protoc. 3, bpy012.

Dircksen, H., 2009. Insect ion transport peptides are derived from alternatively spliced genes and differentially expressed in the central and peripheral nervous system. J. Exp. Biol. 212, 401–412.

Dvoretsky, A.G., Dvoretsky, V.G., 2010. Hemolymph molting hormone concentrations in red king crabs from the Barents Sea. Polar Biol. 33, 1293–1298.

Dvoretsky, A.G., Dvoretsky, V.G., 2016. Inter-annual dynamics of the Barents Sea red king crab (*Paralithodes camtschaticus*) stock indices in relation to environmental factors. Polar Sci. 10, 541–552.
Dvoretsky, A.G., Dvoretsky, V.G., 2020. Effects of environmental factors on the abundance, biomass, and individual weight of juvenile red king crabs in the Barents Sea. Front. Mar. Sci. 7, 726.
Edgar, R.C., 2004. MUSCLE: multiple sequence alignment with high accuracy and high throughput. Nucl. Acids Res. 32, 1792–1797.
Falk-Petersen, J., Renaud, P., Anisimova, N., 2011. Establishment and ecosystem effects of the alien invasive red king crab (*Paralithodes camtschaticus*) in the Barents Sea – a review. ICES J. Mar. Sci. 68, 479–488.
Fang, Y., Diao, L., Zhang, F., Ma, L., Zhao, M., Zhang, D., Sun, M., Pi, Y., Qiao, Z., Jiang, K., 2018. Identification of suitable reference genes of *Scylla paramamosain* for gene expression profiling in various tissues and under vibrio challenge. Crustaceana 91, 1195–1210.
Fanjul-Moles, M.L., 2006. Biochemical and functional aspects of crustacean hyperglycemic hormone in decapod crustaceans: review and update. Comp. Biochem. Physiol. C 142, 390–400.
Foyle, T., O'Dor, R.K., Elner, R., 1989. Energetically defining the thermal limits of the snow crab. J. Exp. Biol. 145, 371–393.
Gao, Y., Zhang, X., Wei, J., Sun, X., Yuan, J., Li, F., Xiang, J., 2015. Whole transcriptome analysis provides insights into molecular mechanisms for molting in *Litopenaeus vannamei*. PLoS One 10, e0144350.
Garland, M.A., Stillman, J.H., Tomanek, L., 2015. The proteomic response of cheliped myofibril tissue in the eurythermal porcelain crab *Petrolisthes cinctipes* to heat shock following acclimation to daily temperature fluctuations. J. Exp. Biol. 2018, 388–403.
Gong, J., Yu, K., Shu, L., Ye, H., Li, S., Zeng, C., 2015. Evaluating the effects of temperature, salinity, starvation and autotomy on molting success, molting interval and expression of ecdysone receptor in early juvenile mud crabs, *Scylla paramamosain*. J. Exp. Mar. Biol. Ecol. 464, 11–17.
Goody, R.T., Gramzowy, L., Battlay, P., Sztal, T., Batterham, P., Robin, C., 2014. The molecular evolution of cytochrome P450 genes within and between *Drosophila* species. Genome Biol. Evol. 6, 1118–1134.
Grabherr, M.G., Haas, B.J., Yassour, M., Levin, J.Z., Thompson, D.A., Amit, I., Adiconis, X., Fan, L., Raychowdhury, R., Zeng, Q., 2011. Full-length transcriptome assembly from RNA-Seq data without a reference genome. Nat. Biotech. 29, 644.
Green, B.S., Gardner, C., Hochmuth, J.D., Linnane, A., 2014. Environmental effects on fished lobsters and crabs. Rev. Fish Biol. Fish. 24, 613–638.
Hall, J.R., Lehnert, S.J., Gonzalez, E., Kumar, S., Hanlon, J.M., Morris, C.J., Rise, M.L., 2020. Snow crab (*Chionoecetes opilio*) hepatopancreas transcriptome: identification and testing of candidate molecular biomarkers of seismic survey impact. Fish. Res. 234, 105794.
Hartnoll, R.G., 1982. Growth. In: Ebele, L.B. (Ed.), The Biology of Crustacea: Embryology, Morphology, and Genetics, 2. Academic Press, New York, pp. 111–196.
Hartnoll, R.G., 2001. Growth in crustacea — twenty years on. Hydrobiologia 449, 111–122.
Hochachka, P.W., Somero, G., 2002. Biochemical Adaptation: Mechanisms and Process in Physiological Evolution. Oxford University Press, New York.
Jeon, J.H., Moon, K.H., Kim, Y.H., Kim, Y.H., 2020. Reference gene selection for qRT-PCR analysis of season- and tissue-specific gene expression profiles in the honey bee *Apis mellifera*. Sci. Rep. 10, 13935.
Jones, D.T., Taylor, W.R., Thornton, J.M., 1992. The rapid generation of mutation data matrices from protein sequences. Comput. Appl. Biosci. 8, 275–282.
Jørgensen, L.L., Primicerio, R., 2007. Impact scenario for the invasive red king crab *Paralithodes camtschaticus* (Tilesius, 1815) (Reptantia, Lithodidae) on Norwegian, native, epibenthic prey. Hydrobiologia 590, 47–54.
Keiler, J., Richter, S., Wirkner, C.S., 2013. Evolutionary morphology of the hemolymph vascular system in hermit and king crabs (Crustacea: Decapoda: Anomala). J. Morphol. 274, 759–778.
Kim, S., Choi, H., Park, J., Min, G., 2013. The complete mitochondrial genome of the subarctic red king crab, *Paralithodes camtschaticus* (Decapoda, Anomura). Mitochondrial DNA 24, 350–352.
Kopylova, E., Noé, L., Touzet, H., 2012. SortMeRNA: fast and accurate filtering of ribosomal RNAs in metatranscriptomic data. Bioinformatics 28, 3211–3217.
Kumar, S., Stecher, G., Li, M., Knyaz, C., Tamura, K., 2018. MEGA X: molecular evolutionary genetics analysis across computing platforms. Mol. Biol. Evol. 35, 1547–1549.
Lachaise, F., Le Roux, A., Hubert, H., Lafont, R., 1993. The molting gland of crustaceans: localization, activity, and endocrine control (a review). J. Crust. Biol. 13, 198–234.
Le, S.Q., Gascuel, O., 2008. An improved general amino acid replacement matrix. Mol. Biol. Evol. 25, 1307–1320.
Lee, K.J., Kim, H.W., Gomez, A.M., Chang, E.S., Covi, J.A., Mykles, D.L., 2007. Molt-inhibiting hormone from the tropical land crab, *Gecarcinus lateralis*: cloning, tissue expression, and expression of biologically active recombinant peptide in yeast. Gen. Comp. Endocrinol. 150, 505–513.
Lindquist, J.A., Mertens, P.R., 2018. Cold shock proteins: from cellular mechanisms to pathophysiology and disease. Cell Commun. Signal. 16, 63.
Liu, G.Y., Sabatini, D.M., 2020. mTOR at the nexus of nutrition, growth, ageing and disease. Nat. Rev. Mol. Cell Biol. 21, 183–203.
Liu, C.J., Huang, S.S., Toullec, J.Y., Chang, C.Y., Chen, Y.R., Huang, W.S., Lee, C.Y., 2015. Functional assessment of residues in the amino-and carboxyl-termini of crustacean hyperglycemic hormone (CHH) in the mud crab *Scylla olivacea* using point-mutated peptides. PLoS One 10, e0134983.
Logan, C.A., Buckley, B.A., 2015. Transcriptomic responses to environmental temperature in eurythermal and stenothermal fishes. J. Exp. Biol. 218, 1915–1924.
Logan, C.A., Somero, G.N., 2010. Transcriptional responses to thermal acclimation in the eurythermal fish *Gillichthys mirabilis* (Cooper 1864). Am. J. Physiol. Reg. Integr. Comp. Physiol. 299, R843–R852.
Long, W.C., Daly, B., 2017. Upper thermal tolerance in red and blue king crab: sublethal and lethal effects. Mar. Biol. 164, 162.
Lorenzon, S., Edomi, P., Giulianini, P.G., Mettulio, R., Ferrero, E.A., 2004. Variation of crustacean hyperglycemic hormone (CHH) level in the eyestalk and haemolymph of the shrimp *Palaemon elegans* following stress. J. Exp. Biol. 207, 4205–4213.
MacLea, K.S., Abuhagr, A.M., Pitts, N.L., Covi, J.A., Bader, B.D., Chang, E.S., Mykles, D. L., 2012. Rheb, an activator of target of rapamycin, in the blackback land crab, *Gecarcinus lateralis*: cloning and effects of molting and unweighting on expression in skeletal muscle. J. Exp. Biol. 215, 590–604.
Manfrin, C., Tom, M., De Moro, G., Gerdol, M., Giulianini, P.G., Pallavicini, A., 2015. The eyestalk transcriptome of red swamp crayfish *Procambarus clarkii*. Gene 557, 28–34.
McCarthy, S.D., Dugon, M.M., Power, A.M., 2015. "Degraded" RNA profiles in Arthropoda and beyond. PeerJ 3, e1436.
Michelsen, H.K., Sparbo, M., Nilssen, E.M., Kettunen, A.H., Siikavuopio, S.I., Christiansen, J.S., 2019. Thermal tolerance of invasive red king crab (*Paralithodes camtschaticus)* larvae from the Barents Sea. In: Shellfish Symposium "Shellfish – Resources and Invaders of the North" (Tromsø, Norway).
Montagné, N., Soyez, D., Gallois, D., Ollivaux, C., Toullec, J.Y., 2008. New insights into evolution of crustacean hyperglycaemic hormone in decapods – first characterization in Anomura. FEBS J. 275, 1039–1052.
Moriyasu, M., Mallet, P., 1986. Molt stages of the snow crab *Chionoecetes opilio* by observation of morphogenesis of setae on the maxilla. J. Crust. Biol. 6, 709–718.
Mykles, D.L., 2011. Ecdysteroid metabolism in crustaceans. J. Steroid Biochem. Mol. Biol. 127, 196–203.
Mykles, D.L., Chang, E.S., 2020. Hormonal control of the crustacean molting gland: Insights from transcriptomics and proteomics. Gen. Comp. Endocrinol. 294, 113493.
Noever, C., Glenner, H., 2018. The origin of king crabs: hermit crab ancestry under the magnifying glass. Zool. J. Linnean Soc. 182, 300–318.
Oliphant, A., Alexander, J.L., Swain, M.T., Webster, S.G., Wilcockson, D.C., 2018. Transcriptomic analysis of crustacean neuropeptide signaling during the moult cycle in the green shore crab, *Carcinus maenas*. BMC Genomics 19, 711.
Oug, E., Cochrane, S.K.J., Sundet, J.H., Norling, K., Nilsson, H.C., 2011. Effects of invasive red king crab, *Paralithodes camtschaticus* on soft-bottom fauna in Varangerfjorden, northern Norway. Mar. Biodivers. 41, 467–479.
Pfaffl, M.W., 2001. A new mathematical model for relative quantification in real-time RT-PCR. Nucl. Acids Res. 29, e45.
Pinchukov, M.A., Sundet, J.H., 2011. In: Jakobsen, T., Ozhigin, V.K. (Eds.), Red King Crab. The Barents Sea. Ecosystem, Resources, Management. Half a Century of Russian-Norwegian Cooperation. Tapir Academic Press, Trondheim, pp. 160–166.
Poloczanska, E.S., Burrows, M.T., Brown, C.J., García Molinos, J., Halpern, B.S., Hoegh-Guldberg, O., Kappel, C.V., Moore, P.J., Richardson, A.J., Schoeman, D.S., Sydeman, W.J., 2016. Responses of marine organisms to climate change across oceans. Front. Mar. Sci. 3, 62.
Pörtner, H.O., 2010. Oxygen- and capacity-limitation of thermal tolerance: a matrix for integrating climate-related stressor effects in marine ectotherms. J. Exp. Biol. 213, 881–893.
Pörtner, H.O., Knust, R., 2007. Climate change affects marine fishes through the oxygen limitation of thermal tolerance. Science 315, 95–97.
Qu, Z., Kenny, N.J., Lam, H.M., Chan, T.F., Chu, K.H., Bendena, W.G., Tobe, S.S., Hui, J. H.L., 2015. How did arthropod sesquiterpenoids and ecdysteroids arise? Comparison of hormonal pathway genes in noninsect arthropod genomes. Genome Biol. Evol. 7, 1951–1959.
Quinn, B.K., 2017. Threshold temperatures for performance and survival of American lobster larvae: a review of current knowledge and implications to modeling impacts of climate change. Fish. Res. 186, 383–396.
Robalino, J., Almeida, J.S., McKillen, D., Colglazier, J., Trent III, H.F., Chen, Y.A., Peck, M.E.T., Browdy, C.L., Chapman, R.W., Warr, G.W., Gross, P.S., 2007. Insights into the immune transcriptome of the shrimp *Litopenaeus vannamei*: tissue-specific expression profiles and transcriptomic responses to immune challenge. Physiol. Genom. 29, 44–56.
Saxton, R.A., Sabatini, D.M., 2017. mTOR signaling in growth, metabolism, and disease. Cell 168, 960–976.
Scheffers, B.R., et al., 2016. The broad footprint of climate change from genes to biomes to people. Science 354, aaf7671.
Shin, S.C., Ahn, D.H., Kim, S.J., Pyo, C.W., Lee, H., Kim, M.K., Lee, J., Lee, J.E., Detrich, H.W., Postlethwait, J.H., Edwards, D., Lee, S.G., Lee, J.H., Park, H., 2014. The genome sequence of the Antarctic bullhead notothen reveals evolutionary adaptations to a cold environment. Genome Biol. 15, 468.
Shyamal, S., Das, S., Guruacharya, A., Mykles, D.L., Durica, D.S., 2018. Transcriptomic analysis of crustacean molting gland (Y-organ) regulation via the mTOR signaling pathway. Sci. Rep. 8, 7307.
Siikavuopio, S.I., James, P., 2015. Effects of temperature on feed intake, growth and oxygen consumption in adult male king crab *Paralithodes camtschaticus* held in captivity and fed manufactured diets. Aquac. Res. 46, 602–608.
Siikavuopio, S.I., Whitaker, R.D., Sæther, B.-S., James, P., Olsen, B.R., Thesslund, T., Hustad, A., Mortensen, A., 2017. First observations of temperature tolerances of adult male snow crab (*Chionoecetes opilio*) from the Barents Sea population and the effects on the fisheries strategy. Mar. Biol. Res. 13, 1745–1819.
Siikavuopio, S.I., Bakke, S., Sæther, B.-S., Thesslund, T., Christiansen, J.S., 2019. Temperature selection and final thermal preferendum of snow crab (*Chionoecetes opilio*) from the Barents Sea. Polar Biol. 42, 1911–1914.

Sokolova, I.M., Frederich, M., Bagwe, R., Lannig, G., Sukhotin, A.A., 2012. Energy homeostasis as an integrative tool for assessing limits of environmental stress tolerance in aquatic invertebrates. Mar. Environ. Res. 79, 1–15.

Squires, H.J., 1990. Decapod crustacea of the Atlantic coast of Canada. In: Can. Bull. Fish. Aquat. Sci. National Government Publication, p. 221.

Sreedhar, A.S., Kalmár, E., Csermely, P., Shen, Y.U., 2004. Hsp90 isoforms: functions, expression and clinical importance. FEBS Lett. 562, 11–15.

Stevens, B.G., 2014. King Crabs on the World, Biology and Fisheries Management. CRC Press, Taylor & Francis Group (608 pp.).

Stiansen, J.E., Korneev, O., Titov, O., Arneberg, P., 2009. Joint Norwegian-Russian environmental status 2008. In: Report on the Barents Sea Ecosystem. Part II–Complete Report. IMR/PINRO Joint Report Series 2009, pp. 1–375.

Stillman, J.H., Fay, S.A., Ahmad, S.M., Swiney, K.M., Foy, R.J., 2020. Transcriptomic response to decreased pH in adult, larval and juvenile red king crab, *Paralithodes camtschaticus*, and interactive effects of pH and temperature on juveniles. J. Mar. Biol. Assoc. U. K 100, 251–265.

Stoner, A.W., Ottmar, M.L., Copeman, L.A., 2010. Temperature effects on the molting, growth, and lipid composition of newly-settled red king crab. J. Exp. Mar. Biol. Ecol. 393, 138–147.

Su, S., Munganga, B.P., Tian, C., Li, J.L., Yu, F., Li, H., Wang, M., He, X., Tang, Y., 2020. Analysis of Intermolt and Postmolt Transcriptomes Provides Insight Into Molecular Mechanisms of the Red Swamp Crayfish, *Procambarus clarkii* Molting. https://doi.org/10.1101/2020.12.09.418467.

Swall, M.E., Benrabaa, S.A.M., Tran, N.M., Tran, T.D., Ventura, T., Mykles, D.L., 2021. Characterization of *Shed* genes encoding ecdysone 20-monooxygenase (CYP314A1) in the Y-organ of the blackback land crab, *Gecarcinus lateralis*. Gen. Comp. Endocrinol. 301, 113658.

Thompson, R.J., Hawryluk, M., 1990. Physiological energetics of the snow crab, *Chionoecetes opilio*. In: Proceedings of the International Symposium on King and Tanner Crabs. Alaska Sea Grant College Program Report, AK-SG-90-04, pp. 283–291.

Tomanek, L., Somero, G.N., 1999. Evolutionary and acclimation-induced variation in the heat-shock responses of congeneric marine snails (genus *Tegula*) from different thermal habitats: implications for limits of thermotolerance and biogeography. J. Exp. Biol. 202, 2925–2936.

Tomanek, L., Somero, G.N., 2002. Interspecific- and acclimation-induced variation in levels of heat-shock proteins 70 (hsp70) and 90 (hsp90) and heat-shock transcription factor-1 (HSF1) in congeneric marine snails (genus *Tegula*): implications for regulation of *hsp* gene expression. J. Exp. Biol. 205, 677–685.

Toullec, J.Y., Corre, E., Mandon, P., Gonzalez-Aravena, M., Ollivaux, C., Lee, C.Y., 2017. Characterization of the neuropeptidome of a Southern Ocean decapod, the Antarctic shrimp *Chorismus antarcticus* : focusing on a new decapod ITP-like peptide belonging to the CHH peptide family. Gen. Comp. Endocrinol. 252, 60–78.

Tudge, C.C., Asakura, A., Ahyong, C.T., 2012. The infraorder Anomura, MacCley 1838. Chapter 70. In: Schram, F.R., von Vaupel Klein, V.C. (Eds.), The Crustacea. Koninklijke Brill NV.

Vandesompele, J., De Preter, K., Pattyn, F., Poppe, B., Van Roy, N., De Paepe, A., Spelman, F., 2002. Accurate normalization of real-time quantitative RT-PCR data by geometric averaging of multiple internal control genes. Genome Biol. 3, 0034.1–0034.11.

Ventura, T., Bose, U., Fitzgibbon, Q.P., Smith, G.G., Shaw, P.N., Cummins, S.F., Elizur, A., 2017. CYP450s analysis across spiny lobster metamorphosis identifies a long sought missing link in crustacean development. J. Steroid Biochem. Mol. Biol. 171, 262–269.

Ventura, T., Palero, F., Rotllant, G., Fitzgibbon, Q.P., 2018. Crustacean metamorphosis: an omics perspective. Hydrobiologia 825, 47–60.

Webster, S.G., 1996. Measurement of crustacean hyperglycaemic hormone levels in the edible crab *Cancer pagurus* during emersion stress. J. Exp. Biol. 199, 1579–1585.

Windisch, H.S., Kathöver, R., Pörtner, H.O., Frickenhaus, S., Lucassen, M., 2011. Thermal acclimation in Antarctic fish: transcriptomic profiling of metabolic pathways. Am. J. Physiol. Regul. Integr. Comp. Physiol. 301, R1453–R1466.

Windisch, H.S., Frickenhaus, S., John, U., Knust, R., Pörtner, H.O., Lucassen, M., 2014. Stress response or beneficial temperature acclimation: transcriptomic signatures in Antarctic fish (*Pachycara brachycephalum*). Mol. Ecol. 23, 3469–3482.

Wittmann, A.C., Storch, D., Anger, K., Pörtner, H.O., Sartoris, F.J., 2011. Temperature-dependent activity in early life stages of the stone crab *Paralomis granulosa* (Decapoda, Anomura, Lithodidae): A role for ionic and magnesium regulation? J. Exp. Mar. Biol. Ecol. 397, 27–37.

Wittmann, A.C., Pörtner, H.O., Sartoris, F.J., 2012. A role for oxygen delivery and extracellular magnesium in limiting cold tolerance of the sub-Antarctic stone crab *Paralomis granulosa*? Physiol. Biochem. Zool. 85, 285–298.

Wittmann, A.C., Benrabaa, S.A.M., López-Cerón, D.A., Chang, E.S., Mykles, D.L., 2018. Effects of temperature on juvenile Dungeness crab, *Metacarcinus magister* (Dana): survival, moulting, and mTOR signalling and neuropeptide gene expression in eyestalk ganglia, moulting gland (Y-organ), and heart. J. Exp. Biol. 221, 187492.

Wolfe, J.M., Breinholt, J.W., Crandall, K.A., Lemmon, A.R., Lemmon, E.M., Timm, L.E., Siddall, M.E., Bracken-Grissom, H.D., 2019. A phylogenomic framework, evolutionary timeline and genomic resources for comparative studies of decapod crustaceans. Proc. R. Soc. B 286, 20190079.

Yamamoto, T., Yamada, T., Kinoshita, T., Ueda, Y., Fujimoto, H., Yamasaki, A., Hamasaki, K., 2015. Effects of temperature on growth of juvenile snow crabs, *Chionoecetes opilio*, in the laboratory. J. Crust. Biol. 35, 140–148.

Yao, T.P., Forman, B.M., Jiang, Z., Cherbas, L., Chen, J.D., McKeown, M., Cherbas, P., Evans, R.M., 1993. Functional ecdysone receptor is the product of EcR and ultraspiracle genes. Nature 366, 476–479.

Zhang, H., Zhao, M., Liu, Y., Zhou, Z., Guo, J., 2018. Identification of cytochrome P450 monooxygenase genes and their expression in response to high temperature in the alligatorweed flea beetle *Agasicles hygrophila* (*Coleoptera: Chrysomelidae*). Sci. Rep. 8, 17847.